Available online at www.sciencedirect.com
SCIENCE DIRECT®
International Journal of Heat and Mass Transfer 49 (2006) 1148–1161
International Journal of HEAT and MASS TRANSFER
www.elsevier.com/locate/ijhmt

Molecular simulations of droplet evaporation processes: Adiabatic pressure jump evaporation

Siswo Sumardiono [1], Johann Fischer *

Institut für Verfahrens- und Energietechnik, Universität für Bodenkultur, Muthgasse 107, A-1190 Wien, Austria

Received 3 February 2005
Available online 7 November 2005

Abstract

For the assessment of droplet evaporation by molecular dynamics simulations prescriptions for the calculation of the time dependent number of droplet particles and of several space and time dependent hydrodynamic quantities like density, drift velocity and temperature are given. Then two cases of adiabatic pressure jump evaporation are treated by molecular simulations using a Lennard-Jones potential. First, a droplet wrapped by its vapour, and second, a bare droplet is brought into vacuum. In both cases evaporation takes place and after a transition process a new droplet-vapour equilibrium is reached at lower temperature. Results are presented for the space and time dependent hydrodynamic quantities as well as for the number of droplet particles as function of time.

1. Introduction

Evaporation and condensation play an important role in energy engineering, in chemical engineering as well as in environmental processes. The use of liquid fuels requires their evaporation outside or inside the combustion chamber. Other frequently used evaporation processes include most drying processes, cooling of water in cooling towers, and cooling of gases by quenching. Evaporation and condensation occur in Rankine and refrigeration cycles as well as in rectification columns. The scientifically interesting aspect of evaporation and condensation processes is that of combined heat and mass transfer and in most cases droplets are involved. Presently there is still a certain tendency in particular in drying technology to model these processes in the framework of fluid mechanics with some adjustable model parameters. We believe, however, that considerations on the molecular scale are required for a full understanding and a physically sound modelling of these processes.

A first molecular approach to describe evaporation and condensation is that by Hertz, Knudsen and Volmer [1–3], who assumed two half-sided Maxwell–Boltzmann (MB) velocity distribution functions outgoing from and incoming to the liquid–vapour interface. The outgoing MB-function has the temperature of the liquid T_l and the density of the saturated vapour $\rho''(T_l)$ at temperature T_l. The incoming MB-function has the temperature T_g and the density of the gas ρ_g. Whilst this model captures already essential features of the physics of evaporation and condensation, details concerning the gas phase, the liquid–gas interface and the liquid phase remained open and deserve more detailed studies. Such studies were performed since about 1960 according to the available theoretical and computational possibilities.

First, the gas phase was studied by using the kinetic theory of gases [4] which allows assessing collisions between the gas molecules. Interesting findings in case of evaporation into vacuum [5] are that about 15% of the evaporated molecules are backscattered to the surface by collisions with other evaporated molecules and that the kinetic temperature in the gas is considerably lower than at the

* Corresponding author. Tel.: +43 1 370 97 26201; fax: +43 1 370 97 26210.
E-mail address: johann.fischer@boku.ac.at (J. Fischer).
[1] Permanent address: Department of Chemical Engineering, Diponegoro University, Semarang, Indonesia.

0017-9310/$ - see front matter © 2005 Elsevier Ltd. All rights reserved.
doi:10.1016/j.ijheatmasstransfer.2005.06.043

evaporating surface. This decrease of the kinetic temperature is easily explained as the temperature is the kinetic energy of the molecules with respect to drift velocity and not with respect to some laboratory coordinate system. The crucial questions with this approach are the initial and the boundary conditions of the velocity distribution function, which are usually modelled as in the Hertz–Knudsen approach as half-sided MB-functions with assumed densities and temperatures.

Regarding the liquid–vapour interface in equilibrium, molecular simulations and theories [6–8] showed for a planar interface of a pure liquid that the density from the liquid to the vapour decreases monotonically and that the interface becomes broader with increasing temperature.

In the next step also evaporation processes from a planar surface were studied by molecular dynamics (MD) [9–12] which is thought to be the key-methodology to validate the assumptions of kinetic theory. In the work of Lotfi [10] steady-state evaporation was considered ranging from maximum evaporation rates for evaporation into vacuum to small evaporation rates in near-equilibrium. The heat required for evaporation was supplied to the liquid by thermostating the bulk some molecular diameters below the onset of the interface at a prescribed temperature T_l. With other words, the heat of evaporation was supplied to the system by coupling the bulk liquid to a heat bath. The most interesting results are described in the following. (a) The density profile changes only marginally in comparison with the equilibrium profile even in case of evaporation into vacuum. (b) At low temperatures, i.e. for $T_l/T_c \approx 0.55$ with T_c being the critical temperature, the thickness of the interface is small and the temperature remains constant from the liquid through the interface till the beginning of the intrinsic vapour. As a consequence, the velocity distribution function of the vapour molecules close to the interface is in agreement with the Hertz–Knudsen assumptions. (c) With increasing temperature, the interface becomes broader and for the case of strong evaporation the temperature drops down already in the interface. At the highest temperature investigated, i.e. for $T_l/T_c \approx 0.85$ the temperature decreases for strong evaporation already in the uppermost layers of the liquid which means that the Hertz–Knudsen model cannot be applied there any longer. (d) Further interesting results concerning the flux of the evaporated particles, the heat flux, the increase of the drift velocity from the liquid through the interface to the vapour and the details of the temperature profiles can be found in the original source [10].

Most evaporation and condensation processes, however, occur via droplets. This inheres non-steady-state or transient processes. Moreover, contrary to the above considered steady-state evaporation, the heat required for droplet evaporation is not delivered to the liquid from a heat bath but must either be supplied by the liquid droplet itself or by the surrounding gas or by both. One example is the cooling of water in a cooling tower, where warm droplets evaporate partially; the heat of evaporation is supplied partly by the droplet and the droplet cools down. An other extreme example is droplets in a combustion process, where the heat of evaporation is supplied by the hot gas in the combustion chamber and the droplets evaporate completely. Besides these two cases there are several different cases as e.g. the evaporation in spray drying. Hence, according to different initial and different boundary conditions there is a variety of transient processes of droplet evaporation. Some of these cases can be treated by applying the Hertz–Knudsen concepts of kinetic theory of gases and interesting work has been done into that direction [13], but this methodology might become cumbersome because the droplet changes size, temperature and in case of mixtures also composition. Other cases like evaporation in combustion chambers can presumably not at all be treated in this way because the droplet is likely to be heated up to temperatures close to the critical, where Lotfi [10] has shown the breakdown of the Hertz–Knudsen concept. Hence, it is quite natural to use molecular dynamics simulations also to study the evaporation of droplets. Quantities of interest are e.g. the density profile, the temperature profiles in radial and tangential direction, the drift velocity, and the heat and mass flux depending on different initial and boundary conditions. In the case of mixtures which occur e.g. in spray drying particular interest lies also in the concentration profiles and the mass transport of the evaporating component inside the droplet.

At this point it is helpful to introduce the cut and shifted Lennard-Jones potential using the cut-off radius r_c

$$u(r) = u_{LJ}(r) - u_{LJ}(r_c) \quad \text{for } r < r_c, \tag{1a}$$

$$= 0 \quad \text{for } r > r_c, \tag{1b}$$

where u_{LJ} is the usual Lennard-Jones (LJ) potential

$$u(r) = 4\varepsilon[(\sigma/r)^{12} - (\sigma/r)^6]. \tag{2}$$

Throughout this paper reduced temperatures and reduced particle densities are used according to $T^* = kT/\varepsilon$ and $\rho^* = \rho\sigma^3$. Moreover, the time unit is $\tau = (m\sigma^2/\varepsilon)^{1/2}$ and the simulation time steps are measured as $\Delta t^* = \Delta t/\tau$. For convenience, the stars are omitted where no confusion can occur. Most frequently, the cut-off radius is chosen to be $r_c = 2.5$ and we simply call the corresponding cut and shifted LJ potential LJ2.5. The vapour–liquid phase equilibria of the non-confined LJ2.5 system have been discussed already in the literature [8,14–16]. We want to point out in particular that the critical temperature of the LJ2.5 fluid is $T_c^* = 1.085$ [14], which is remarkably lower than that of the LJ fluid without cut-off found to be $T_c^* = 1.31$ [14,17]. An estimate for the triple point temperature T_{tr}^* can be made on the basis of real argon, for which $T_{tr} = 83.80\,\text{K}$ and $T_c = 150.687\,\text{K}$, and hence $T_{tr}/T_c = 0.556$. Assuming the same ratio yields $T_{tr}^* = 0.60$ for the LJ2.5 fluid. Moreover, because of the considerably lower critical temperature of the LJ2.5 fluid the coexistence curve properties of the LJ2.5 fluid are remarkably different [8,14–16] from those of the LJ fluid [14,17] at the same

reduced temperature T^*. In particular, the saturated vapour densities of the LJ2.5 fluid are higher by a factor of 3 than those of the LJ fluid in a large temperature range of interest.

Before considering evaporation of liquid droplets, an understanding of droplets in equilibrium is necessary. The first molecular simulation of liquid droplets in equilibrium seems to be that of Rusanov and Brodskaya [18]. A milestone was then the MD study of liquid drops by Thompson et al. [19]. In this work the atoms interact with the LJ2.5 potential and the simulations were performed at either constant energy or constant temperature. The quantities calculated at different temperatures and for different droplet sizes are the density profile $\rho(r)$, the normal and tangential components of the pressure tensor $p_N(r)$ and $p_T(r)$, the surface thickness, the equimolar radius R_e and the surface tension γ; a detailed discussion on the calculation of the surface tension is included.

There are two findings in the Thompson et al.'s work [19] which are of particular interest for evaporation studies. One finding is that the equilibrium gas densities surrounding the droplets are considerably higher than the saturated vapour densities of the LJ-fluid without cut-off [17] with differences ranging up to an order of magnitude. One reason already mentioned is that the saturated vapour densities of the LJ2.5 fluid are higher by a factor of 3 than those of the LJ fluid in the temperature range considered. An other reason is that according to the Kelvin equation the vapour pressure and hence also the saturated vapour density increases for a drop. An other important finding of the Thompson et al.'s work [15] is that rather long equilibration periods are needed.

After the very careful simulation studies on droplets in equilibrium and the evaporation from a plane surface, MD-simulations on the evaporation of droplets were made by other groups. The first paper known to us is that of Long et al. [20]. These authors considered a LJ2.5 droplet surrounded by its vapour in a box at temperature $T^* = 0.65$. In order to achieve evaporation, those molecules which reached the boundary regions of the box were heated up there to the temperature $T^* = 1.00$. Besides several pictures showing the droplet during evaporation the main quantitative result of this paper is that the droplet diameter is a linear function of the evaporation time. In a subsequent paper [21] of the same group two topics were addressed. First, it was shown for a pure LJ2.5 fluid that the number of droplet particles as function of evaporation time obtained with initially N_1 droplet molecules and those obtained with initially N_2 molecules agree by appropriate scaling. Second, the vaporization of a liquid oxygen drop into a hydrogen or a helium environment was studied using between 5000 and 10,000 oxygen molecules and a total number of molecules which is approximately four times higher. The initial configurations were achieved by equilibrating the droplet and the environment separately and then combining the results. The oxygen droplet was at saturation at 100 K and the hydrogen or helium environment at 200 or 300 K and pressures up to 20 MPa. During the evaporation process the systems were kept at the environmental pressure. Moreover, as heat is transferred to the droplet the gas molecules were heated up to the initial environmental temperature in the boundary regions of the box as before. Quantitative results are the number of molecules in a droplet, the droplet temperature, and the oxygen mole fraction as function of the radial distance from the droplet center, all as functions of time. Much emphasis is put on the different behaviour of the droplet at subcritical and supercritical pressures. At subcritical pressures the droplet remains spherical and retains a distinct temperature profile throughout the entire vaporization process. In contrast, at supercritical pressures the droplet vaporizes in a cloud-like manner with vanishing surface tension. The latter was determined by an ad hoc estimation based on the averaged attractive force on the drop particles. Two additional papers of the same group review existing results and present additional atomisation phenomena [22] and deal again with scaling [23].

In an other paper on droplet evaporation Bhansali et al. [24] studied a LJ system forming a drop and its surrounding vapour till equilibrium was achieved at a prescribed temperature. Then they increased the prescribed temperature and allowed the system to equilibrate at this higher temperature. In this manner they achieved a series of drop-vapour equilibria at five temperatures and recorded equilibrium properties like density profiles, pressures and surface tensions. Unfortunately little information about the intrinsic evaporation process is given.

The concepts of Long et al. [20] were taken up again by Walther and Koumoutsakos [25] who investigated the subcritical evaporation of mostly LJ2.5 droplets into their own vapour. One of the aims of this work was to extend the MD-algorithms to large particle numbers. This is achieved with an "adaptive tree data structure" for the construction of the neighbor lists. Actually, droplet evaporation simulations with initially up to 51,105 liquid and 105,480 vapour particles are reported. The systems were prepared such that initial configurations were taken from fcc lattices with liquid and vapour densities corresponding to real bulk argon and a droplet is cut from the lattice into a spherical shape. This initial configuration is said to have been equilibrated at a subcritical temperature $T_l^* = 0.83$ over 5000–10,000 time steps of length $\Delta t^* = 0.005$ which the present authors consider as a remarkably short equilibration period. Thereafter, the vapour was heated up outside a sphere being some distance away from the drop surface to the temperature $T_\infty = 3T_l$. The droplet then started to evaporate. Reported results are density and temperature profiles, droplet diameters and evaporation coefficients. In the present authors opinion the real merit of this paper is the development of the adaptive tree data structure. Regarding the physical considerations, however, there are points which are not easy to understand. The first is the preparation and equilibration of the droplet. As the initial vapour density was taken as the saturated vapour density of real bulk

argon it is according to the above discussion of previous findings [8,15–17] at least three times too low for a LJ2.5 droplet in equilibrium with its vapour. As the initial number of vapour particles was between two and six times higher than that of the droplet particles, more than the available droplet particles would have been needed to equilibrate the system. Hence, as the vapour density was considerably below saturation, the droplet should have started to evaporate already without being heated by the vapour. With this background it is rather difficult to understand why evaporation of the LJ2.5 droplet is reported to start only at $T^* = 1.16$ which is higher than the critical temperature $T_c^* = 1.085$ of the LJ2.5 fluid [14–16]. A potential explanation for this high evaporation temperature could be the rather unconventional definition of the "temperature" in this paper which was defined as the kinetic energy in the laboratory system without taking into account the drift velocity. The latter, however, can become very high in the vapour and in the interface during evaporation [10]. Finally, even if this temperature definition problem can be resolved, the fact remains that evaporation was driven simultaneously by the vapour density being far below the saturation density as well as by the heat transferred to the drop. Whilst such "mixed cases" occur frequently in technical processes it seems rather difficult to draw unique conclusions for modeling from such case studies.

The last and most recent MD-study on evaporation of droplets known to us is that by Consolini et al. [26]. They investigated the evaporation of an initially pure droplet of xenon into an ambient vapour of nitrogen at subcritical and supercritical conditions. Initial subcritical state conditions are for the drop $T = 165$ and $\rho = 2600\ \mathrm{kg/m^3}$ and for the ambient gas 330, 650 and 1030 K, respectively, and $\rho = 8.5\ \mathrm{kg/m^3}$. The study is similar to that of Kaltz et al. [21] where also a cold droplet was put into hot vapour with the difference that Kaltz et al. heated up the vapour molecules whenever they reached the boundaries of the simulation box whilst Consolini do not transfer additional energy to the system. The MD results are shown in essence to be independent of the droplet and system sizes considered, which confirms earlier findings of Kaltz et al. [21] for evaporation of a pure fluid into its own vapour. An other interesting finding is that at subcritical conditions the droplet tends to stay spherical or to become spherical for initial non-spherical shape. A certain difference with respect to Kaltz et al. [21] is in the history of the droplet temperature at subcritical conditions. Whilst Kaltz et al. found continuous increase of the drop temperature, the present authors find a certain saturation temperature; this difference is likely to be caused by the fact that Kaltz et al. kept the temperature constant at the boundaries and hence added continuously energy to the system. For the supercritical case the droplet does not return to the spherical shape and its temperature increases continuously during the "vaporization" process.

Summarizing we can say that the available MD studies on evaporation of droplets have given some interesting results. They also show, however, as could have been expected that the results depend strongly on the initial and boundary conditions and a variety of cases remain to be explored. Of course, there was some interest to arrive as soon as possible at the evaporation of a liquid droplet into an ambient vapour of different molecules. The simpler case, however, is that of evaporation of a droplet in a single component system. After the above discussion we believe that several phenomena remain to be investigated for the single component case in more detail.

Several initial and boundary value problems are conceivable in a single component system for evaporation of a droplet. For convenience in terminology we distinguish whether a droplet is in equilibrium with its vapour—we call this a wrapped droplet—or whether a sphere has been simply cut out from a homogeneous liquid—we call this a bare droplet. Without being complete, we can distinguish the following cases. Case 1: A wrapped droplet is put together with its vapour into vacuum. Case 2: A bare droplet is cut out and put into vacuum. Cases 1 and 2 have some physical similarity and are summarized as "adiabatic pressure jump evaporation". Case 3: Start from a cold wrapped droplet and heat the vapour in some distance from the droplet (case of Long et al. [20]). Case 4: Put a cold bare droplet into hot vapour and add energy to the system. This case was considered by Kaltz et al. [21] but for vapour molecules being of different type than the liquid molecules at the beginning of the simulation. Cases 3 and 4 have some physical similarity and are summarized as "continuous heat transfer evaporation". Case 5: Put a cold bare droplet into hot vapour without adding energy to the system. This case was considered by Consolini et al. [26] but for vapour molecules being of different type than the liquid molecules at the beginning of the simulation. Case 6: Consider a liquid drop surrounded by non-saturated vapour of equal temperature and heat up the vapour which is the "mixed" case considered by Walther and Koumoutsakos [25].

It is the purpose of this paper to extend the study of Lotfi [10] for steady-state evaporation from a plane surface to the transient evaporation of drops in single component systems. In particular, we will study here the "adiabatic pressure jump evaporation" corresponding to Cases 1 and 2. The "continuous heat transfer evaporation" corresponding to Cases 3 and 4 will be the subject of a subsequent paper. The studies on adiabatic pressure jump evaporation can be considered as a first model for describing the cooling of water in cooling towers.

2. Model and properties definitions

The model fluid considered here is the cut and shifted Lennard-Jones fluid with a potential cut-off distance $r_c = 2.5\sigma$, which we call LJ2.5.

The definitions of the potential have been given above in Eqs. (1a), (1b) and (2). The LJ2.5 potential is chosen (1) because the potential has to be cut off in any case in the molecular dynamics simulations, (2) long-range corrections

are tedious for spherical drops, (3) most droplet simulations have been done for that potential, and (4) vapour–liquid phase equilibria of the non-confined LJ2.5 system have been discussed already in the literature [8,14–16] and were shortly summarized in Section 1.

The preparation of the simulation runs requires detailed descriptions depending on different initial and boundary conditions. The common starting point is to prepare a homogeneous liquid at prescribed temperature T_l and density ρ_l by placing initially all atoms at the sites of a face center cubic (FCC) lattice in a cube of box length L_l. Usual numbers of atoms consistent with the fcc lattice are $N_c = 32$, 108, 256, 500, 864, 1372, 2048. Then an equilibration run is performed at NVT conditions over 20,000 time steps of length $\Delta t^* = 0.005$ which is used throughout the paper. Assuming for m, σ and ε the usual parameters for argon $\Delta t^* = 0.005$ corresponds to 10.75 fs. In the same way a homogeneous vapour is prepared in a separate system at T_v and ρ_v. Traditionally, we use for the integration of the equations of motion the fifth order predictor corrector algorithm presented by Gear [27] and recommended by Haile [28,29]. The temperature is kept constant by rescaling the velocities of all particles such that the total kinetic energy E_{kin} remains constant.

In a next step, a spherical droplet is created by cutting out the atoms contained in the largest possible sphere of the "liquid" cube. As the volume of the sphere is $(4\pi/3)(L_l/2)^3$ the average number of initial particles in the droplet is $N_0 = (\pi/6)N_c = 0.524N_c$. The particles of the liquid droplet retain their positions with respect to the center of the sphere and also their velocities. This droplet is then placed depending on the case study either into the center of an empty box or into the center of a box with vapour. In the latter case the vapour molecules have to be removed from the sphere occupied by the droplet. The vapour can have the same or a different temperature as the liquid depending again on the case studied.

After the system has been prepared so far, it is helpful for the following to define whether an atom belongs to the droplet or to the vapour. For that purpose, several definitions are available in the literature [19–21,24,25,30]. In essence, three groups of definitions can be distinguished, two of which were given by Thompson et al. in [19] as "Cornell" and "Oxford" definition and the third is that of Rein ten Wolde and Frenkel [30].

In the "Cornell" definition a molecule j is said to be within the droplet at the time t provided that the condition $r_{ij} \leqslant R_{cl}$ was fulfilled, where molecule i is known to be in the cluster and R_{cl} is a suitably chosen length. The algorithm is entered with $i = 1$, where molecule 1 is the one closest to the last known position of the center of mass of the droplet and is thus known to be "in the droplet". In the first step we look for those molecules j for which r_{ij} obeys $r_{ij} \leqslant R_{cl}$. Having located the molecules in the first shell, the sorting procedure starts in the second step from any of the molecules in the first shell and looks for molecules k connected to any of the j molecules with $r_{jk} \leqslant R_{cl}$. Those molecules k which have not yet been counted before as belonging to the droplet form the second shell. This procedure is continued until one does not find any more molecules connected to the droplet. The number of the particles belonging to the droplet is N_d and the center of the droplet is calculated. In practice R_{cl} was set equal to 1.542σ.

In the "Oxford" definition molecule i is taken to be in the droplet at time t if there are at least n_c molecules of type j such that r_{ij} obeyed $r_{ij} \leqslant R_{cl}$, with $R_{cl} = 2.5\sigma$. The number n_c is varied from 7 to 4 as the temperature rose from $T^* = 0.63$–0.8; these numbers are significantly less than the mean number of molecules expected to be in a sphere of radius 2.5σ in the uniform liquid.

The definition of Rein ten Wolde and Frenkel [30] is similar to the "Oxford" definition with the differences that $R_{cl} = 1.5$ which corresponds to the first minimum in the radial distribution function of the liquid and that the number n_c is taken to be 4. It contains still a second criterion which is important for the study of nucleation but does not seem to us to be very relevant for evaporation and hence is neglected here. Henceforth, we understand as "Amsterdam" definition: a particle j is a nearest neighbor to i if $r_{ij} \leqslant R_{cl} = 1.5\sigma$ and particle i belongs to the droplet if it has at least $n_c = 4$ nearest neighbors.

From a physical point of view the Cornell definition is the most satisfying but it is computationally most intensive. It might be necessary to use that definition in case that the droplet completely disappears. For pressure jump evaporation, however, where the droplet survives the Amsterdam and Oxford definition seem to be equally well suited. Here, we will mainly work with the Amsterdam definition but compare the result in one case also with the Cornell definition.

Using such a definition it is possible to label at a given time each particle as belonging to the droplet (d) or to the vapour (v) and to count the number of atoms in the droplet N_d. For the following, it is helpful to define the center of the drop $\mathbf{r}_{cd}$ as

$$\mathbf{r}_{cd} = (1/N_d)\sum_{i\mathrm{d}} \mathbf{r}_{i\mathrm{d}}, \tag{3}$$

where the summation goes over all droplet particles. Moreover, we will also use the notion of the center of mass of the whole system

$$\mathbf{r}_{cm} = (1/N)\sum_{i} \mathbf{r}_i. \tag{4}$$

Keeping in mind that the number of atoms in the droplet N_d is a function of time t, $N_d(t)$, a net particle evaporation flux j can be defined as net number of particles which pass from the droplet to the vapour per unit surface area and a specified time interval $\Delta\tau$

$$j(t) = [N_d(t) - N_d(t + \Delta\tau)]/A\Delta\tau, \tag{5}$$

where A is the droplet surface area. The time interval $\Delta\tau$ has to be specified with some care. On the one hand $\Delta\tau$ should be larger than the integration time step Δt in order

to avoid a sensitivity to instantaneous fluctuations and on the other hand it should allow a certain time resolution. In the present paper we will not calculate $j(t)$ because the droplets considered consist only of some hundred particles and hence statistics are not sufficiently accurate in order to calculate $j(t)$. Eq. (5) is given here for methodological completeness.

If the molecules belonging to the droplet are well defined, it is helpful for all further evaluations to fix the center of the cubic box in the center of the droplet $\mathbf{r}_{cd}$. In addition to the number of particles in the droplet $N_d(t)$ and the evaporation flux $j(t)$, quantities of interest are the local density ρ, the radial drift velocity v_D, the total kinetic energy of the system E_{kin}, the mean kinetic energy per particle e_{kin}, as well as the radial temperature T_r, the tangential temperature T_t and the total temperature T. Note that the quantities ρ, v_D, e_{kin}, T_r, T_t, and T all are functions of the radial distance r from the center of the drop and of the time t. We assume that the droplets remain spherically symmetric during the evaporation process which at least seems to hold on a coarse grained time scale, i.e. by averaging over several hundreds or thousands time steps of length Δt.

The density profile $\rho(r)$ in the droplet, the vapour–liquid interface and the surrounding vapour was calculated up to $1/2L_l$, i.e. up to half the box length, by determining time averaged numbers of atoms in spherical shells. Let the radii of the spheres be $r_1, r_2, \ldots, r_{n-1}, r_n, \ldots$, the number of particles in the nth shell be N_n, its time average be $\langle N_n \rangle$, and the volume of the nth shell be V_n, then the local density $\rho(r)$ is given by

$$\rho(r) = \langle N_n \rangle / V_n \tag{6}$$

and assigned to the radius r

$$r = [1/2(r_n^3 - r_{n-1}^3)]^{1/3}. \tag{7}$$

The time averaging periods depend on whether the system was in equilibrium or in a transient state and will become clear in the context of the particular case.

Using that shell concept, also the drift velocity and the temperatures were determined. For the drift velocity we assume for reasons of spherical symmetry that it only has a radial component. Let us start with considering some particle i which has position $\mathbf{r}_i$ and velocity $\mathbf{v}_i$ with both quantities being vectors. Now let us decompose the velocity $\mathbf{v}_i$ into a radial velocity $\mathbf{v}_{ir}$ and a tangential velocity $\mathbf{v}_{it}$. This can be done by introducing a radial unit vector $\mathbf{e}_r$ defined by $\mathbf{r}_i/r_i$ with $r_i = |\mathbf{r}_i|$. Therewith, the radial velocity $\mathbf{v}_{ir}$ and the tangential velocity $\mathbf{v}_{it}$ are given as

$$\mathbf{v}_{ir} = (\mathbf{v}_i \cdot \mathbf{e}_r)\mathbf{e}_r, \tag{8}$$

$$\mathbf{v}_{it} = \mathbf{v}_i - \mathbf{v}_{ir}. \tag{9}$$

Moreover, we need the radial velocity component

$$v_{ir} = (\mathbf{v}_i \cdot \mathbf{e}_r), \tag{10}$$

which can be positive or negative. Now, let us consider all particles i_n in the nth shell Therewith the radial drift velocity $v_D(r)$ in the nth shell is given as

$$v_D(r) = \left\langle 1/N_n \sum_{in} v_{in,r} \right\rangle, \tag{11}$$

where the summation goes over all particles i_n in the nth shell and $\langle \cdots \rangle$ denotes appropriate time averaging. We note, that $v_D(r)$ can be positive or negative.

With this notation the instantaneous total kinetic energy of the system is given by

$$E_{kin} = (m/2) \sum_i \mathbf{v}_i^2 \tag{12}$$

and the mean kinetic energy per particle $e_{kin}(r)$ in the nth shell is given by

$$e_{kin}(r) = \left\langle (m/2N_n) \sum_{in} \mathbf{v}_{in}^2 \right\rangle, \tag{13}$$

where the summation again goes over all particles i_n in the nth shell and $\langle \cdots \rangle$ denotes appropriate time averaging.

The temperature is given according to the kinetic theory of gases via the squared random velocity which is obtained from the actual velocity by subtracting the drift velocity. Hence, we define the random part $\mathbf{v}_{ig}$ of the velocity $\mathbf{v}_i$ as

$$\mathbf{v}_{ig} = \mathbf{v}_i - v_D \mathbf{e}_r \tag{14}$$

and the random part $\mathbf{v}_{ih}$ of the radial velocity $\mathbf{v}_{ir}$ as

$$\mathbf{v}_{ih} = \mathbf{v}_{ir} - v_D \mathbf{e}_r. \tag{15}$$

Therewith, the "radial" temperature $T_r(r)$ is given as

$$T_r(r) = (m/k) \left\langle 1/N_n \sum_{in} v_{in,h}^2 \right\rangle, \tag{16}$$

which can be rewritten by using Eqs. (15) and (11) as

$$T_r(r) = (m/k) \left[\left\langle 1/N_n \sum_{in} v_{in,r}^2 \right\rangle - v_D^2 \right], \tag{17}$$

if the same time averaging interval $\langle \cdots \rangle$ is used in Eqs. (11) and (17). Similarly, the "tangential" temperature $T_t(r)$ is given as

$$T_t(r) = (m/2k) \left\langle 1/N_n \sum_{in} v_{in,t}^2 \right\rangle \tag{18}$$

and the total temperature $T(r)$ as

$$T(r) = (m/3k) \left\langle 1/N_n \sum_{in} v_{in,g}^2 \right\rangle, \tag{19}$$

where the summation goes over all particles i_n in the nth shell and $\langle \cdots \rangle$ denotes appropriate time averaging. Combining Eqs. (17)–(19) we get

$$T = 1/3T_r + 2/3T_t. \tag{20}$$

Finally, from Eqs. (13), (14) and (19) we get the relation between the temperature T and the kinetic energy per particle e_{kin} as

$$(3/2)kT = e_{kin} - (m/2)v_D^2. \tag{21}$$

3. Equilibration of the droplet with its vapour

Whilst the main purpose of this paper is the study of evaporation, there are two cases, Cases 1 and 3, in which the evaporation shall start from a droplet in equilibrium with its vapour which we call a wrapped droplet. Hence, it seems appropriate to discuss the preparation of a wrapped droplet be sure that the intended initial condition has been achieved. We remind that such studies have already been made [19,31] and the message is that special attention has to be paid to the preparation and equilibration of the droplets.

Here, we consider as an example a usual, non-optimized equilibration to obtain a droplet in equilibrium with its vapour at $T = 0.80$. For this purpose we may start with a NVT simulation of a homogeneous liquid in a cubic box with periodic boundary conditions for $N = 1372$ particles at a density $\rho = 0.80$ which is the saturated liquid density of the full LJ system [17]; the liquid box length is $L_\mathrm{l} = 11.97$. Next, we run a NVT simulation of a homogeneous vapour for 108 particles at a density $\rho = 0.010$ which is somewhat higher than the saturated vapour density of the full LJ system found to be $\rho'' = 0.006$; the vapour box length is $L_\mathrm{v} = 22.10$. Each of these runs is performed over 20,000 time steps. Next, a spherical droplet is created by cutting out the atoms contained in the largest possible sphere of the liquid cube which yields 724 "liquid" particles; the radius of this sphere is $R_L = L_\mathrm{l}/2 = 5.98$. The same sphere is then cut out from the center of the vapour cube which leaves 95 "vapour" particles in the remaining volume (vapour cube minus liquid sphere). The liquid and vapour are then merged in the vapour box by placing the spherical liquid droplet into the empty sphere in the center of the vapour box. In those simulation codes in which the box length is taken as unit length, the remaining vapour molecules retain their positions and velocities, whilst for the liquid molecules a rescaling is necessary for the reduced positions $\mathbf{x} = \mathbf{r}/L$ according to

$$\mathbf{x}_{i,\mathrm{new}} = 0.5 + (\mathbf{x}_{i,\mathrm{old}} - 0.5)(L_\mathrm{l}/L_\mathrm{v}), \tag{22}$$

and similarly for the reduced velocities $\mathbf{w} = (\mathbf{v}/L)(\Delta t/\sigma)$ according to

$$\mathbf{w}_{i,\mathrm{new}} = \mathbf{w}_{i,\mathrm{old}}(L_\mathrm{l}/L_\mathrm{v}). \tag{23}$$

At this point we have to repeat that the saturation properties of the LJ2.5 fluid are different from those of the LJ fluid. At $T = 0.80$, we have for the full LJ fluid $\rho' = 0.80$ and $\rho'' = 0.006$ [17], whilst for the LJ2.5 fluid the corresponding values are $\rho' = 0.73$ and $\rho'' = 0.020$ [16]. Hence, in the above prepared merged liquid vapour system the vapour density is too low by a factor of 2 whilst the liquid density is about 10% too high. As a consequence, equilibration of the merged system means now already evaporation.

In these equilibration runs, the total kinetic energy of the system E_kin is kept constant by rescaling the velocities with E_kin being fixed to $3/2NkT$ with $T = 0.8$. An interesting point is now to consider the mean kinetic energy per particle $e_\mathrm{kin}(r)$ in different concentric shells around the center of the droplet. The simulation shows that at the beginning of the equilibration the mean kinetic energy per particle is in the liquid drop lower than E_kin/N and in the vapour phase higher than E_kin/N. The reason for this behavior is that the flow of evaporating particles has a drift velocity which strongly contributes to the kinetic energy. In this connection we repeat our warning that the kinetic energy of a non-equilibrium system must not be taken as measure for the temperature. The correct calculation of the temperature requires subtraction of the drift velocity from the particle velocities as in Eqs. (14) and (19). In general, after a certain equilibration time, the mean kinetic energy per particle in the shells should become constant throughout the system and equal to $E_\mathrm{kin}/N = 3/2kT$.

During the equilibration there are several quantities to be observed in order to decide whether the system has reached equilibrium. Frequently it is said that a stable local density profile according to Eq. (6) has to be reached. This is true with the addition that the most sensitive part of the density profile is the vapour density remote from the drop which needs the longest time to arrive at a stable value. In our particular example we obtained in the center of the droplet a "liquid" density $\rho_\mathrm{l} = 0.74$ and in the vapour $\rho_\mathrm{v} = 0.030$ with the averaging done from time step 75,000 to time step 85,000. We note that the vapour density outside the curved droplet is higher than the saturated vapour density for the non-confined LJ2.5 system being $\rho'' = 0.020$, whilst the droplet density agrees with the saturated liquid density $\rho' = 0.73$ within the simulation uncertainties. A second criterion concerns the mean kinetic energy per particle in the shells $e_\mathrm{kin}(r)$ which should become spatially constant and equal to $3/2kT$. A third criterion is the mean displacement x_mean of the particles from the center of mass

$$x_\mathrm{mean} = (1/L_\mathrm{v})\left[1/N\sum_i(\mathbf{r}_i - \mathbf{r}_\mathrm{cm})^2\right]^{1/2}. \tag{24}$$

In the particular example we observed that x_mean started with 0.27, increased after 75,000 time steps Δt up to 0.36 and thereafter oscillated between this value and 0.34.

After all, the statement remains that the preparation of the wrapped droplet requires some care and remarkably long simulation runs.

4. Adiabatic pressure jump evaporation studies

Pressure jump evaporation in a general sense means that for a system containing liquid and eventually vapour the pressure is suddenly decreased and as a consequence the liquid evaporates [32]. Several initial and boundary conditions are conceivable. Here two related cases will be studied in which no energy is transferred to the system after the pressure jump, hence we call them adiabatic pressure jump evaporation studies. First a wrapped droplet together with its vapour is put into vacuum, second a bare droplet is put into vacuum.

4.1. Evaporation of a wrapped droplet

The starting point is a droplet in equilibrium with its vapour. The system consists of 819 particles in a box of $L_1 = 22.10$ and has been equilibrated at $T = 0.80$ as has been described in Section 3. This system was put into a larger box which was initially empty. The larger boxes have box lengths L_2 with $L_2/L_1 = 1.5$ and $L_2/L_1 = 2.0$. First we consider the case $L_2/L_1 = 1.5$ in detail, thereafter we report some results for $L_2/L_1 = 2.0$. We remind that placing the smaller box into the larger box requires in a code where the box length is taken as unit length again position and velocity rescaling according to Eqs. (22) and (23).

The behavior which we expect is that the system expands into the larger volume and part of the droplet will evaporate. In order to leave the potential energy well of the droplet the particles need energy. As the system is treated adiabatically, this energy must be supplied from the total kinetic energy. This means that the system temperature will go down and consequently the density of the liquid droplet will increase and the density of the vapour phase will decrease. After a certain transition time the system should find a new equilibrium at a lower temperature.

As a check we estimated the temperature T_2 in the new equilibrium state on the basis of the conservation of energy. The initial system indexed with 1 has N particles in a box of volume $V_1 = L_1^3$ at temperature $T_1 = 0.80$ and its total energy is U_1. Now we assume for simplicity that at any temperature T the liquid drop has the density $\rho'(T)$ and the internal energy $u'(T)$ of the saturated liquid and the surrounding vapour has the corresponding quantities $\rho''(T)$ and $u''(T)$ of the saturated vapour of the LJ2.5 fluid. These quantities are known from [16]. Then we can calculate on the basis of the conservation of mass and energy the equilibrium state in the larger volume $V_2 = L_2^3$. With this procedure we found for $L_2/L_1 = 1.5$ the new equilibrium temperature $T_2 = 0.703$ and for $L_2/L_1 = 2.0$ the new equilibrium temperature $T_2 = 0.640$.

4.1.1. Simulation results for $L_2/L_1 = 1.5$

The preparation of the system in its initial equilibrium state in the box with length L_1 ($L_1 = 22.10$) has been discussed in Section 3. Then this system is placed into the larger box with length L_2 ($L_2 = 33.15$) and its transition from the initial to the final equilibrium is observed.

Fig. 1 shows the local density ρ as function of the distance r from the droplet center for the equilibrium before evaporation and for two time periods after onset of evaporation, i.e. after the wrapped droplet has been brought into the larger box. The calculations were done according to Eq. (6) by using spherical shells. The local density profiles show as usual three different regions. The first region is the liquid phase, the second is the liquid–vapour interface and the third region is the vapour phase. The density profiles are shown first because they give an impression about the size of the liquid droplet and the thickness of the interface. The local density shows some scattering near the center of the droplet because the number of particles in the spherical shells becomes small in approaching the center. Let us first look on the density profile at the initial equilibrium at $T = 0.80$. There, the density in the droplet is $\rho_l = 0.74$ and in the vapour it is $\rho_v = 0.030$ as already stated in Section 3. For the further discussion of Fig. 1 we must anticipate that the system cools down during evaporation. Consequently the liquid density should increase, the vapour density decrease and the liquid–vapour interface should become thinner. Actually we see that in the second profile averaged over time steps 6001–8000 after onset of evaporation the density in the droplet increases to $\rho_l = 0.80$ and in the vapour it decreases to $\rho_v = 0.0108$. Finally, in the third profile averaged over time steps 15,001–25,000 after onset of evaporation the density in the droplet increases to $\rho_l = 0.82$ and in the vapour it decreases to $\rho_v = 0.0106$. This last density profile does not change any more when the simulation run is continued until 150,000 time steps.

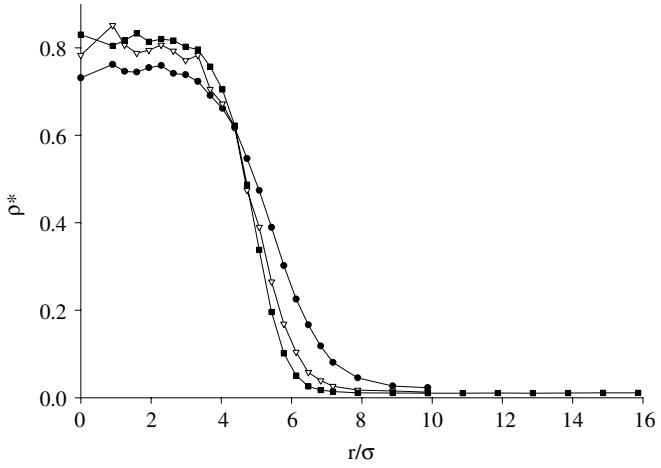

Fig. 1. Reduced local density ρ^* as function of the reduced distance r/σ from the droplet center for different time periods for evaporation of a wrapped droplet by expansion of the volume ($L_2/L_1 = 1.5$). (—●—) initial equilibrium, (—▽—) averaged over time steps 6001–8000 after onset of evaporation, (—■—) averaged over time steps 15,001–25,000 after onset of evaporation.

In Fig. 2 the radial drift velocities v_D are presented which have been calculated according to Eq. (11). Shown is the reduced drift velocity v_D^* which is related to the physical quantity v_D by $v_D^* = (m/\varepsilon)^{1/2} v_D$. In order to get a feeling for the reduced velocities we note that for a half-sided MB velocity distribution v_D^* takes the value $v_D^* = ((2/\pi)T^*)^{1/2}$ which e.g. for $T^* = 0.8$ yields $v_D^* = 0.71$; the ideal gas sound velocity of a monatomic gas at $T^* = 0.8$ is $c^{id_*} = 1.15$. Drift velocity profiles are shown for different time periods after onset of evaporation with all periods having a length of 2000 time steps. We note that immediately after the wrapped droplet has been brought into the larger box the vapour expands very rapidly with a drift velocity which comes close to the drift velocity of a half-sided MB-velocity distribution which could have been expected. The droplet itself has zero drift velocity. An

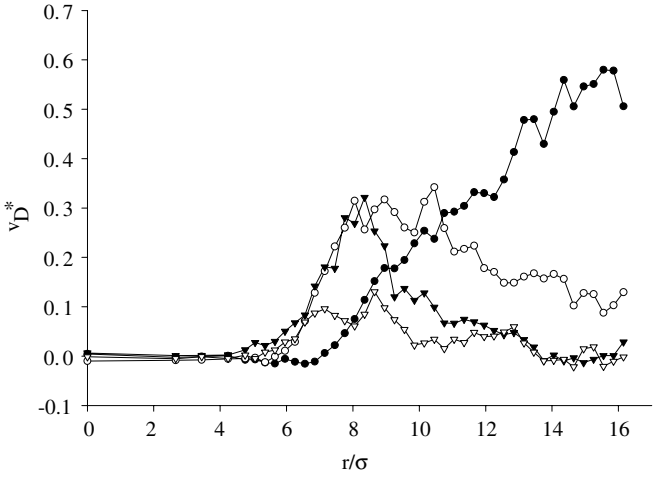

Fig. 2. Reduced radial drift velocity v_D^* as function of the reduced distance r/σ from the droplet center for different time periods for evaporation of a wrapped droplet by expansion of the volume ($L_2/L_1 = 1.5$). (—●—) averaged over time steps 1–2000, (—○—) averaged over time steps 2001–4000, (—▼—) averaged over time steps 8001–10,000, (—▽—) averaged over time steps 18,001–20,000 after onset of evaporation.

interesting feature is that at the distance $r/\sigma \approx 7$ the drift velocity has a slight negative value, i.e. the particles in the liquid–vapour interface move inside. This recoil effect is in some sense an effect of local momentum conservation and we remind that in ''Laser-Pellet-Fusion'' this is the main effect for getting high pellet densities. In the time period from 2001 to 4000 time steps there occurs a change in the drift velocity. The recoil frontier moves a little towards the droplet center and a larger part of the interface starting from distance $r/\sigma \approx 6$ moves rapidly outside where the particles find now new free space. At further remote distances the drift velocity decreases in comparison with that at the beginning of the evaporation. We explain this by the fact that particles from the replica box move into the central box and that by this move the velocities between the outgoing and incoming particles cancel out to some extent in the calculation of the drift velocity such that this decreases. The third profile for the time period from 8001 to 10,000 time steps is a continuation of the behaviour found in the second time period. Finally, in the period from 18,001 to 20,000 time steps the drift velocity tends to zero as a consequence of the fact that the system approaches its new equilibrium.

After having obtained the radial drift velocity v_D it is possible to calculate the radial temperature T_r, the tangential temperature T_t and the total temperature T according to Eqs. (17)–(19). We remind that Eq. (17) requires the same time averaging interval for T_r and v_D; this means that $v_{in,r}^2$ and $v_{in,r}$ are averaged simultaneously during the simulation run. Results for T_r, and T_t are shown in Fig. 3, whilst the total temperature T is shown in Fig. 4.

First we learn from Fig. 4(a) that the temperature of the liquid and of the vapour in equilibrium as function of the distance from the droplet center is rather constant around the value 0.8, which was achieved by prescribing the total

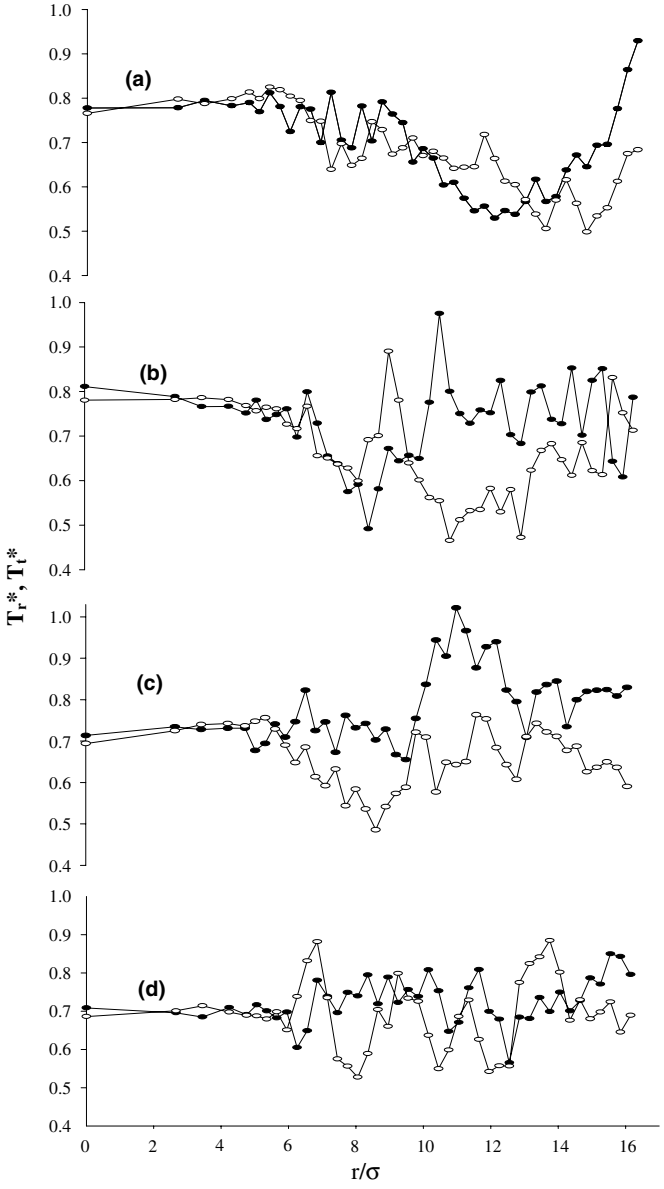

Fig. 3. Reduced radial temperature T_r^* (—●—) and reduced tangential temperature T_t^* (—○—) as function of the reduced distance r/σ from the droplet center for different time periods for evaporation of a wrapped droplet by expansion of the volume ($L_2/L_1 = 1.5$). (a) Averaged over time steps 1–2000, (b) averaged over time steps 2001–4000, (c) averaged over time steps 4001–6000, (d) averaged over time steps 8001–10,000 after onset of evaporation.

kinetic energy of the system to be $E_{kin}/\varepsilon = (3N/2)T^*$ with $T^* = 0.8$.

Then, evaporation starts and T_r and T_t for the first 2000 time steps are shown in Fig. 3(a), whilst the total temperature T is given in Fig. 4(b). Looking on T_r we note that inside the droplet and in the liquid–vapour interface the radial temperature fluctuates around a value which is slightly lower than the equilibrium temperature $T = 0.8$; here and in the following reduced temperature values are given. In the vapour phase, however, the radial temperature decreases down to $T_r = 0.52$ at the distance $r/\sigma = 12$. This decrease had to be expected on the assumption that

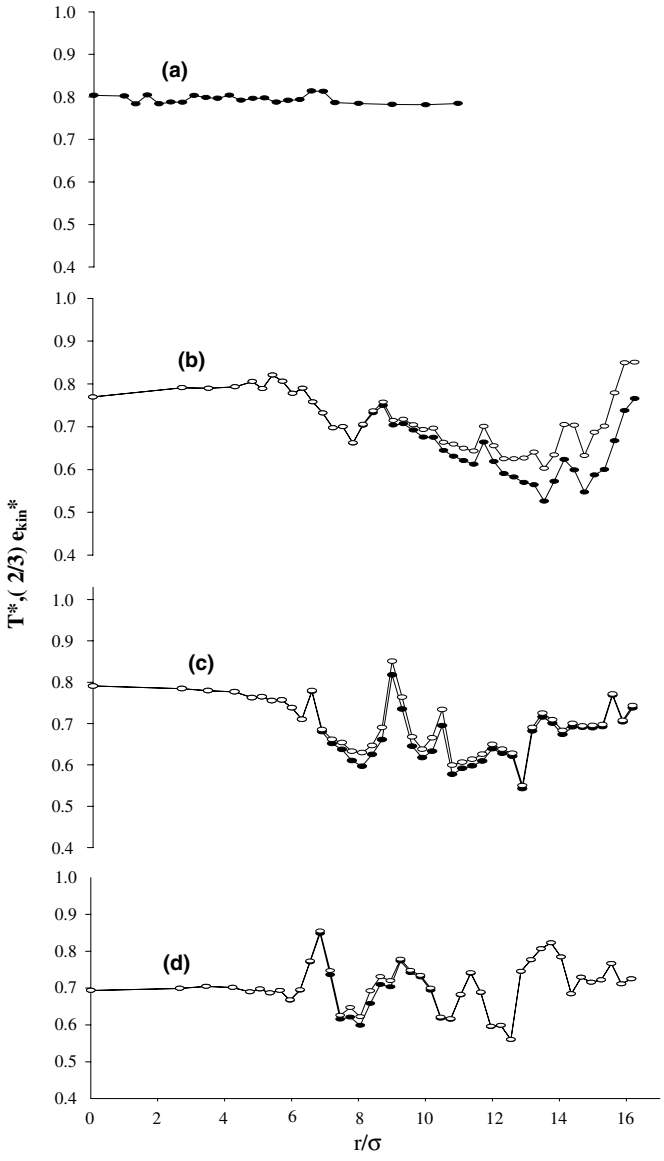

Fig. 4. Reduced total temperature T^* (—●—) and corresponding reduced mean kinetic energy per particle $(2/3)e^*_{kin}$ (—○—) as function of the reduced distance r/σ from the droplet center for different time periods for evaporation of a wrapped droplet by expansion of the volume ($L_2/L_1 = 1.5$). (a) Equilibrium, (b) averaged over time steps 1–2000, (c) averaged over time steps 2001–4000, (d) averaged over time steps 8001–10,000 after onset of evaporation.

a half-sided MB distribution function moves outward. What is not completely understood is the strong increase of the radial temperature at the boundary of the box. We conjecture that this is an effect of the particles moving from the replica into the central box. Looking now on T_t we see that it shows a similar behaviour as T_r with low values for r/σ between 13 and 16. This is somewhat surprising because from the work of Lotfi [10] we had expected T_t to remain near its initial equilibrium value. Anyhow, the findings suggest that there is strong interaction between the velocity components. The total temperature T is according to Eq. (20) a linear combination of T_r and T_t, $T = 1/3T_r + 2/3T_t$, and consequently we find in Fig. 4(b) values of T lower than 0.6 for r/σ between 13 and 15.

In the next time period from 2001 to 4000 time steps, shown in Fig. 3(b), T_r remains inside the droplet in essence constant but the minimum of T_r moves into the liquid–vapour interface. The surprising fact is the increase of T_r to a value of nearly 1.0 at the distance $r/\sigma = 10.5$. The tangential temperature T_t shows also one peak and two minima with rather low values for r/σ between 9 and 15. The total temperature T, presented in Fig. 4(c), shows one pronounced maximum around $r/\sigma = 9$ and two minima around $r/\sigma = 8$ and $r/\sigma = 12$ with $T \approx 0.6$.

Results for T_r and T_t in the third period from 4001 to 6000 time steps are shown in Fig. 3(c). Both become nearly constant at a value between 0.70 and 0.75 inside the droplet and in the interface. The surprising facts, however, are the high value of T_r up to 1.0 around $r/\sigma = 11$ whilst T_t drops down to 0.5 around $r/\sigma = 8$ which indicates a rather dynamic behaviour in the gas phase.

For the period from 8001 to 10,000 time steps results are given in Fig. 3(d) and Fig. 4(d). The system approaches its final equilibrium with the temperature being close to $T = 0.70$ but with still strong fluctuations in the vapour. We remind that 0.70 is close to the value 0.703 estimated above from the conservation of energy.

It is now of some interest to look at the mean kinetic energy per particle e_{kin} defined in Eq. (13) which is related to the temperature T via Eq. (21), which in reduced quantities can be rewritten as $(2/3)e^*_{kin} = T^* + (1/3)v^{*2}_D$. Hence, e_{kin} can already be obtained by combining the drift velocity from Fig. 2 with the temperature from Fig. 4. For convenience of the reader, we show e_{kin} in the form $(2/3)e^*_{kin}$ also in Fig. 4. Trivially, a large difference between both quantities happens for large values of v_D which occur in particular at the onset of evaporation in the vapour phase. Hence, we observe the largest differences between e_{kin} and T in Fig. 4(b).

Finally, we show in Fig. 5 the number of droplet particles as function of time during the evaporation process calculated according to the Amsterdam definition. We note, that after the initial equilibration process the droplet consists of about 480 liquid particles. Then during pressure jump evaporation by increase of the box length with ratio $L_2/L_1 = 1.5$ the number of particles decreases to 405, which is a decrease by about 16%. The decrease can within statistical uncertainties approximately be described as exponential with a change to horizontal between 100 and 150 ps corresponding to 9000–14,000 time steps. But even thereafter we observe some fluctuations in the particle number which correlate with the fact that the drift velocity shown in Fig. 2 is not yet completely zero in the time period from 18,001 to 20,000 time steps.

4.1.2. Simulation results for $L_2/L_1 = 2.0$

Starting from $L_1 = 22.10$, $L_2 = 44.20$. The results obtained for this case are qualitatively similar to those for $L_2/L_1 = 1.5$. We show here only the number of droplet

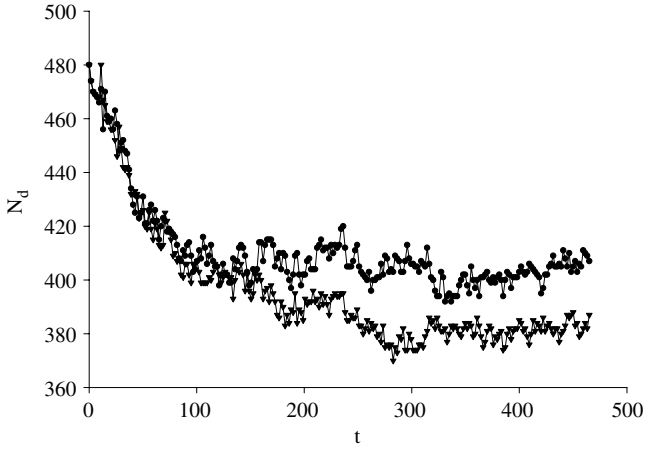

Fig. 5. Number of droplet particles N_d as function of time t in picoseconds for evaporation of a wrapped droplet by expansion of the volume (1 ps corresponds to 93 time steps). (—●—) $L_2/L_1 = 1.5$, (—▼—) $L_2/L_1 = 2.0$ (both according to Amsterdam definition).

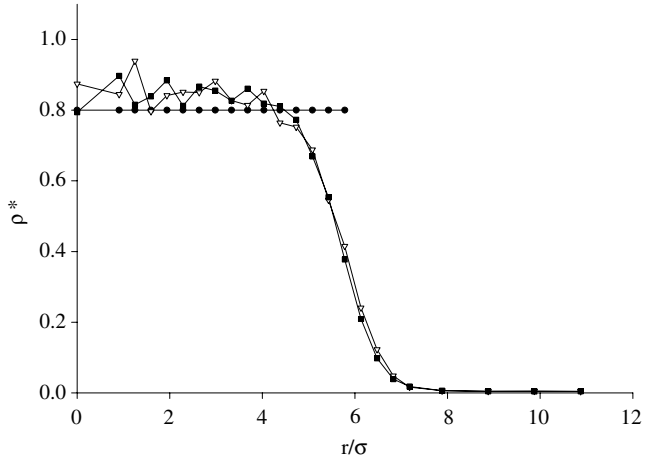

Fig. 6. Reduced local density ρ^* as function of the reduced distance r/σ from the droplet center for different time periods for evaporation of a bare droplet into vacuum. (—●—) initial droplet, (—▽—) averaged over time steps 6001–8000 after onset of evaporation, (—■—) averaged over time steps 15,001–25,000 after onset of evaporation.

particles as function of time according to the Amsterdam definition which is given in Fig. 5. We learn that the initial decrease in droplet particles is nearly the same for $L_2/L_1 = 2.0$ as for $L_2/L_1 = 1.5$ but the decrease lasts longer for $L_2/L_1 = 2.0$. The final number of about 380 droplet particles is reached after about 300 ps corresponding to 28,000 time steps which is a decrease by about 21%. Again, the final temperature $T = 0.6497$ is very close to the value 0.640 estimated above from the conservation of energy.

4.2. Evaporation of a bare droplet

Here, the initial droplet is the sphere which was cut out from a bulk liquid as described in Section 3. The starting point there was a NVT simulation of a homogeneous liquid in a cubic box with periodic boundary conditions for $N = 1372$ particles at temperature $T = 0.80$. The liquid box length is $L_1 = 11.97$ resulting in a density $\rho = 0.80$ which is the saturated liquid density of the full LJ system. Next, a spherical droplet is created by cutting out the atoms contained in the largest possible sphere of the liquid cube which yields 724 "liquid" particles.

This bare spherical liquid droplet with 724 particles (droplet radius $R_L = L_1/2 = 5.98$) is then put into an empty box with box length L_2 with $L_2/L_1 = 2.0$ ($L_2 = 23.94$). First, the system is thermostated at $T = 0.80$ for 400 time steps, thereafter it is treated adiabatically and the expected behaviour is similar to that obtained above. An estimate of the temperature T_2 in the final equilibrium was made again on the basis of conservation of energy as above. Because of the liquid density $\rho = 0.80$ the internal energy $u(T, \rho)$ is not taken from [16] but rather from the own initial bulk fluid simulation. The resulting value is $T_2 = 0.663$.

Fig. 6 shows the local density ρ as function of the distance r from the droplet center for the equilibrium before evaporation and for two time periods after onset of evaporation. Again, the system cools down and the liquid density increases. The profiles are shown for the time steps 6001–8000 and 15,001–25,000 after onset of evaporation. The latter density profile does not change any more when the simulation is continued.

In Fig. 7 the radial drift velocities v_D are presented. We observe a qualitatively similar behaviour as for the evaporation of the wrapped drop with, however, larger values of the drift velocity. Note that the drift velocity values in the first time period reach a value of about $v_D^* = 1.00$ which is larger than the value 0.71 resulting from a half-sided MB distribution at the temperature $T = 0.8$. This indicates that the bare liquid droplet with its high density and without being in equilibrium with is vapour expands more quickly into the vacuum. One might compare this with the drift

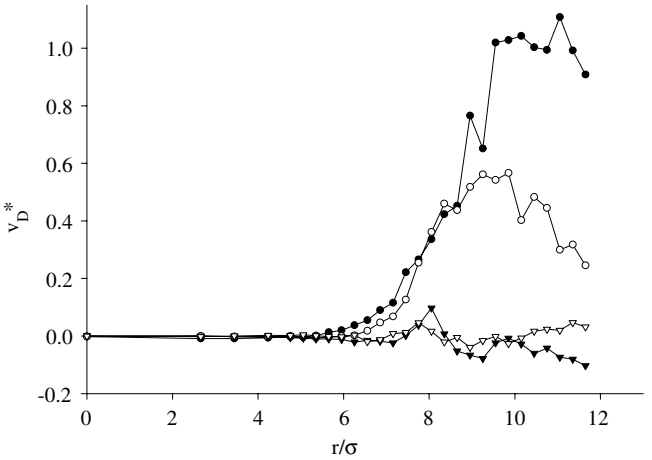

Fig. 7. Reduced radial drift velocity v_D^* as function of the reduced distance r/σ from the droplet center for different time periods for evaporation of a bare droplet into vacuum. (—●—) averaged over time steps 1–2000, (—○—) averaged over time steps 2001–4000, (—▼—) averaged over time steps 8001–10,000, (—▽—) averaged over time steps 18,001–20,000 after onset of evaporation.

velocity found by Lotfi [10] who obtained for $T = 0.85$ a drift velocity $v_D^* = 0.90$, which is also above the drift velocity 0.73 of the half sided MB distribution for $T = 0.85$. We do not observe negative drift velocities at the beginning of the evaporation but in the course of the time they are found in the remote gas phase which we understand as dynamical fluctuations in the vapour.

In Fig. 8 the radial temperature T_r and the tangential temperature T_t are shown, whilst in Fig. 9 the total temperature T is presented and the mean kinetic energy per particle e_{kin}. The qualitative behaviour here is in general the same as for the evaporation of the wrapped drop shown in Figs. 3 and 4. There are, however, a few differences that should be addressed. One observation is that the temperature in the droplet decreases for the bare droplet in the

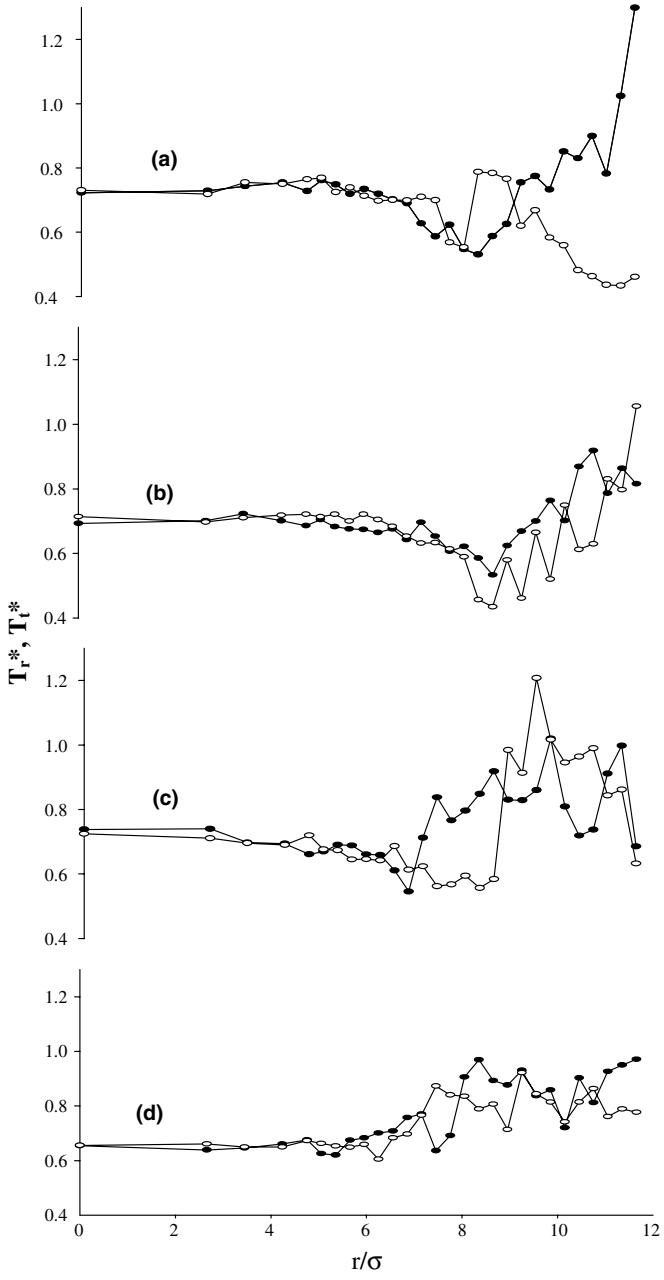

Fig. 8. Reduced radial temperature T_r^* (—●—) and reduced tangential temperature T_t^* (—○—) as function of the reduced distance r/σ from the droplet center for different time periods for evaporation of a bare droplet into vacuum. (a) Averaged over time steps 1–2000, (b) averaged over time steps 2001–4000, (c) averaged over time steps 4001–6000, (d) averaged over time steps 8001–10,000 after onset of evaporation.

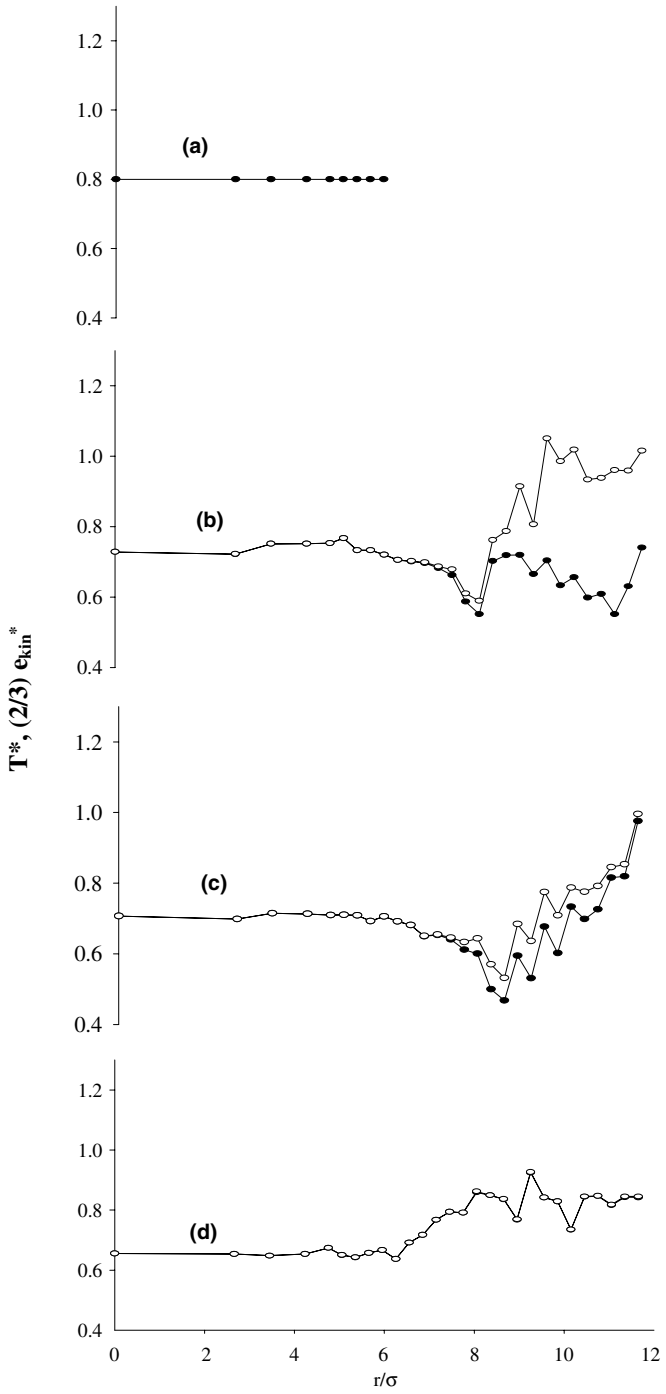

Fig. 9. Reduced total temperature T^* (—●—) and corresponding reduced mean kinetic energy per particle $(2/3)e_{kin}^*$ (—○—) as function of the reduced distance r/σ from the droplet center for different time periods for evaporation of a bare droplet into vacuum. (a) Equilibrium, (b) averaged over time steps 1–2000, (c) averaged over time steps 2001–4000, (d) averaged over time steps 8001–10,000 after onset of evaporation.

beginning more rapidly than for the wrapped droplet as can be seen e.g. by comparison of Fig. 8(b) with Fig. 4(b). We attribute this to the fact that in the wrapped droplet first the already existing vapour shell expands and only thereafter molecules will leave the droplet which requires energy from the droplet. In case of the bare droplet, however, the molecules which fill the vacuum have to leave the droplet and hence the temperature decreases in the beginning more rapidly. Next, we see from Fig. 9(d) that for the bare droplet evaporation in the period from 8001 to 10,000 time steps the temperature in the vapour is thoroughly higher than in the droplet which indicates that full equilibrium has not yet been achieved. For the wrapped droplet evaporation we observe from Fig. 4(d) for the same time period the same average temperature in the vapour and in the liquid. Moreover, on the basis of Fig. 9(b) we want to point out the large difference between the temperature and the corresponding kinetic energy in the vapour. Finally, we want to point out that there is again good agreement of the temperature in the liquid from the simulation found to be $T = 0.67$ in comparison with the value $T = 0.663$ found from the energy balance.

Finally, we show in Fig. 10 the number of droplet particles as function of time during the evaporation process calculated according to the Amsterdam definition and according to the Cornell definition. We note, that the initial droplet consists of 724 liquid particles. According to the Amsterdam definition, the number of particles decreases finally to 590, which is a decrease by 19%. According to the Cornell definition, the number of particles decreases finally to 620, which is a decrease by 14%. Generally, the droplet has more particles according to the Cornell definition. This can be easily understood because particles which are connected with the center of the droplet only by one near neighbour are counted by Cornell as belonging to the droplet whilst in the Amsterdam definition at least four near neighbours are required.

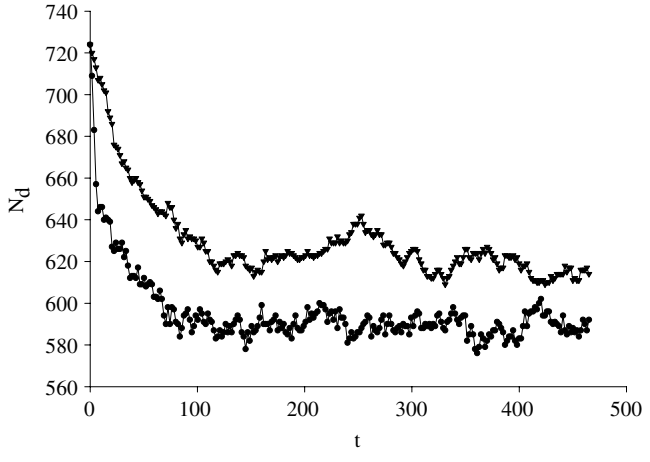

Fig. 10. Number of droplet particles N_d as function of time t in picoseconds for evaporation of a bare droplet into vacuum (1 ps corresponds to 93 time steps) according to Amsterdam (—●—) and Cornell definition (—▼—).

5. Summary and outlook

In this paper we have first reviewed thoroughly existing literature on droplets and evaporation. Next, we have introduced a detailed concept for the description of a droplet in a transient process. This includes the definition of the number of particles N_d belonging to the droplet which is a time dependent quantity. This concept also explains how to calculate the hydrodynamic quantities as the density profile, the drift velocity, the radial, the tangential and the total temperature and the mean kinetic energy per particle and the relations between these quantities are given. These hydrodynamic quantities depend in case of a transient process on the distance from the droplet center and on the evaporation time. Then two cases of adiabatic pressure jump evaporation were studied: the evaporation of a wrapped droplet and that of a bare droplet into vacuum. Both cases show some general similarity. In adiabatic pressure jump evaporation the temperature of the droplet has to decrease which corresponds to approaching the "temperature at the wet bulb". The simulations show that the final temperatures could be estimated reasonably well from appropriately chosen equilibrium data by using the first law of thermodynamics. The real new insights concern the details about the transition from the initial to the final equilibrium state and in particular the time scales for these processes. We believe that it will not be easy to describe this phenomena by a theory without using molecular dynamics simulation results.

In several cases we compared our results with those obtained by Lotfi [10] for the steady-state evaporation from a plane liquid surface into vacuum. In general there was reasonable agreement between the findings. One point for future clarification is the behaviour of the tangential temperature. Whilst in the steady-state evaporation study of Lotfi the tangential temperature remained constant through the interface, it decreases in the vapour phase to rather low temperatures in case of transient droplet evaporation.

We believe that the present study gave a first insight into transient pressure jump droplet evaporation. There remain, however, many questions to be investigated of which we want to mention only two. One problem is that our droplets are rather small and one should go to larger droplets which, obviously, requires a more efficient simulation methodology. A second problem of some technological interest is the evaporation of mixture-droplets.

Acknowledgements

The authors thank Dr.-Ing. Jadran Vrabec, Institut für Technische Thermodynamik und Thermische Verfahrenstechnik, Universität Stuttgart, and Dr.-Ing. Martin Wendland, Institut für Verfahrens- und Energietechnik, Universität für Bodenkultur Wien, for many fruitful discussions. The authors also acknowledge gratefully that J. Vrabec, Gaurav Kumar Kedia, G. Fuchs and H. Hasse

from Universität Stuttgart have made available their results from Ref. [16] prior to publication.

One of us (S.S.) gratefully acknowledges a fellowship in the program ASEA-Uninet sponsored by Österreichische Akademische Austauschdienst (Austrian Academic Exchange Service) and the European Union.

References

[1] H. Hertz, I. Über die Verdunstung der Flüssigkeiten, insbesondere des Quecksilbers, im luftleeren Raume, Ann. Phys. 253 (1882) 177.
[2] M. Knudsen, Die maximale Verdampfungsgeschwindigkeit des Quecksilbers, Ann. Phys. 352 (1915) 697.
[3] M. Volmer, Kinetik der Phasenbildung, Steinkopff-Verlag, Dresden, Leipzig, 1939.
[4] M.N. Kogan, Rarefied Gas Dynamics, Plenum Press, New York, 1969.
[5] J. Fischer, Distribution of pure vapour between two parallel plates under the influence of strong evaporation and condensation, Phys. Fluids 19 (1976) 1305.
[6] J.S. Rowlinson, B. Widom, Molecular Theory of Capillarity, Clarendon Press, Oxford, 1982.
[7] J. Fischer, M. Methfessel, Born–Green–Yvon approach to the local densities of a fluid at interfaces, Phys. Rev. A 22 (1980) 2836.
[8] A. Lotfi, J. Vrabec, J. Fischer, Orthobaric densities from simulations of the liquid vapour interface, Mol. Simul. 5 (1990) 233.
[9] A. Lotfi, J. Fischer, MD-simulation results for the dynamics in the liquid–vapour interface, Ber. Bunsen-Ges. Phys. Chem. 94 (1990) 294.
[10] A. Lotfi, Molekulardynamische Simulationen an Fluiden: Phasengleichgewicht und Verdampfung, Ph.D. thesis at Ruhr-Universität-Bochum Germany 1993, Fortschritt-Berichte VDI, VDI-Verlag Düsseldorf, 1993 (ISBN 3-18-143503-1). Available from: <http://www.map.boku.ac.at/2906.html>.
[11] K. Yasuoka, M. Matsumoto, Y. Kataoka, Evaporation and condensation at a liquid surface, I. Argon. J. Chem. Phys. 101 (1994) 7904–7911.
[12] M. Matsumoto, K. Yasuoka, Y. Kataoka, Molecular simulation of evaporation and condensation, Fluid Phase Equilibria 104 (1995) 431–439.
[13] G.F. Hubmer, U.M. Titulaer, Heat transfer between a small sphere and a dilute gas: the influence of the kinetic boundary layer, Physica A 171 (1991) 337–349.
[14] B. Smit, Phase diagrams of Lennard-Jones fluids, J. Chem. Phys. 96 (1992) 8639–8640.
[15] W. Shi, J.K. Johnson, Histogram reweighting and finite-size scaling study of the Lennard-Jones fluids, Fluid Phase Equilibria 187–188 (2001) 171–191.
[16] J. Vrabec, G.K. Kedia, G. Fuchs, H. Hasse, Comprehensive study on vapor–liquid coexistence including planar and spherical interface properties of the truncated and shifted Lennard-Jones fluid, in preparation.
[17] A. Lotfi, J. Vrabec, J. Fischer, Vapour liquid equilibria of the Lennard-Jones fluid from the $NpT+$ test particle method, Mol. Phys. 76 (1992) 1319.
[18] A.I. Rusanov, E.N. Brodskaya, The molecular dynamics simulation of a small drop, J. Colloid Interface Sci. 62 (1977) 542.
[19] S.M. Thompson, K.E. Gubbins, J.P.R.B. Walton, R.A.R. Chantry, J.S. Rowlinson, A molecular dynamics study of liquid drops, J. Chem. Phys. 81 (1984) 530–542.
[20] N.L. Long, M.M. Micci, B.C. Wong, Molecular dynamics simulation of droplet evaporation, Comput. Phys. Commun. 96 (1996) 167–172.
[21] T.L. Kaltz, L.N. Long, M.M. Micci, J.K. Little, Supercritical vaporization of liquid oxygen droplets using molecular dynamics, Combust. Sci. Technol. 136 (1998) 279–301.
[22] M.M. Micci, T.L. Kaltz, L.N. Long, Molecular dynamics simulations of atomization and spray phenomena, Atomization Sprays 11 (2001) 351–363.
[23] M.M. Micci, T.L. Kaltz, L.N. Long, Molecular dynamics simulations of micrometer-scale droplet vaporization, Atomization Sprays 11 (2001) 653–666.
[24] A.P. Bhansali, Y. Bayazitoglu, S. Maruyama, Molecular dynamics simulation of an evaporating sodium droplet, Int. J. Therm. Sci. 38 (1999) 66–74.
[25] J.H. Walther, P.J. Koumoutsakos, Molecular dynamics simulation of nanodroplet evaporation, J. Heat Transfer 123 (2001) 741–748.
[26] L. Consolini, S.K. Aggarwal, S. Murad, A molecular dynamics simulation of droplet evaporation, Int. J. Heat Mass Transfer 46 (2003) 3179–3188.
[27] C.W. Gear, Numerical Initial Value Problems in Ordinary Differential Equations, Prentice Hall Inc., Englewood Cliffs, NJ, 1971.
[28] J.M. Haile, A primer on the computer simulation of atomic fluids by molecular dynamics, Script, Clemson University, Clemson, SC, 1980.
[29] J.M. Haile, Molecular Dynamics, Elementary Methods, Wiley, New York, 1992.
[30] P. Rein ten Wolde, D. Frenkel, Computer simulation study of gas–liquid nucleation in a Lennard-Jones system, J. Chem. Phys. 109 (1998) 9901–9918.
[31] M.J.P. Nijmeijer, C. Bruin, A.B. von Woerkom, A.F. Bakker, Molecular dynamics of the surface tension of a drop, J. Chem. Phys. 96 (1992) 565–576.
[32] F.W. Schulze, H.K. Cammenga, Investigation of phase transition kinetics liquid–vapour by a pressure-jump relaxation technique, Ber. Bunsen-Ges. Phys. Chem. 84 (1980) 163–168.